The EPIC Crop Growth Model

J. R. Williams, C. A. Jones, J. R. Kiniry, D. A. Spanel

ABSTRACT

The EPIC plant growth model was developed to estimate soil productivity as affected by erosion throughout the U.S. Since soil productivity is expressed in terms of crop yield, the model must be capable of simulating crop yields realistically for soils with a wide range of erosion damage. Also, simulation of many crops is required because of the wide variety grown in the U.S. EPIC simulates all crops with one crop growth model using unique parameter values for each crop. The processes simualted include leaf interception of solar radiation; conversion to biomass; division of biomass into roots, above ground mass, and economic yield; root growth; water use; and nutrient uptake. The model has been tested throughout the U.S. and in several foreign countries.

INTRODUCTION

Recently, a mathematical model called EPIC (Erosion-Productivity Impact Calculator) was developed to determine the relationship between soil erosion and soil productivity in the U.S. (Williams et al., 1984). EPIC is composed of physically based components for simulating erosion, plant growth, and related processes. It also includes economic components for assessing the cost of erosion, determining optimal management strategies, etc. The physical processes involved are simulated simultaneously and realistically using readily-available inputs. Since erosion can be a relatively slow process, EPIC is capable of simulating hundreds of years if necessary.

The EPIC model was used to analyze the relationships among erosion, productivity, and fertilizer needs as part of the Soil and Water Resources Conservation Act (RCA) analysis for 1985. EPIC provided erosion-productivity relationships for about 900 benchmark soils and 500,000 crop/tillage/conservation strategies throughout the U.S. Thus, the model had to be generally applicable, computationally efficient, and capable of computing the effects of management decision. Model components include weather simulation, hydrology, erosion-sedimentation, nutrient cycling, crop growth, tillage, soil temperature, economics, and plant environment control. Several of these components have been described elsewhere (Williams et al., 1984; Jones et al., 1984a, 1984b; Jones, 1985; Sharpley et al., 1984).

Only one of the model components, crop growth, is described here. Since soil productivity is expressed in terms of crop yield, crop growth is one of the most important processes simulated by EPIC. To evaluate the effect of erosion on crop yield, the model must be sensitive to crop characteristics, weather, soil fertility, and other soil properties. The processes simulated include crop interception of solar radiation; conversion of intercepted light to biomass; division of biomass into roots, above-ground biomass, and economic yield; root growth; water use; and nutrient uptake. Potential plant growth is simulated daily and constrained by the minimum of five stress factors (water, nitrogen, phosphorus, temperature, and aeration). Root growth is constrained by the minimum of three stress factors (soil strength, temperature, and aluminum toxicity). Through its effects on soil properties and plant and root growth stress factors, erosion affects crop production indirectly.

EPIC simulates all crops with one crop growth model using unique parameter values for each crop. EPIC is capable of simulating crop growth for both annual and perennial plants. Annual crops grow from planting to harvest date or until the accumulated heat units equal the potential heat units for the crop. Perennial crops (alfalfa, grasses, and pine trees) maintain their root systems throughout the year, although the plant may become dormant after frost. They start growing when the average daily air temperature exceeds the base temperature of the plant.

The EPIC crop table contains parameter values for soybeans, alfalfa, corn, grain sorghum, wheat, barley, oats, sunflower, cotton, pasture, peanuts, potatoes, Durham wheat, winter peas, faba beans, rapeseed, sugarcane, sorghum hay, range grass, rice, cassava, lentils, and pine trees.

MODEL DESCRIPTION

The framework of an early version of the EPIC crop model was described previously (Williams et al., 1984). The model has been modified, expanded, and tested extensively since that time. Thus, the objectives here are to describe in detail the 1988 version of the EPIC crop model and to present test results for several crops and locations.

Phenological development

The phenological development of plants is accelerated

Article was submitted for publication in March, 1988; reviewed and approved for publication by the Soil and Water Div. of ASAE in November, 1988.

Contribution from the USDA-Agricultural Research Service, in cooperation with Texas Agricultural Experiment Station, Texas A&M University System.

The authors are: J.R. WILLIAMS, Hydraulic Engineer, USDA-Agricultural Research Service; C.A. JONES, Professor, TAES; J.R. KINIRY, Research Agronomist; and D.A. SPANEL, Biological Technician, USDA-Agricultural Research Service, Temple, TX.

Acknowledgment: The measured data represent work by researchers from several disciplines in several countries (Table 1). Their willingness to share this information is deeply appreciated.

by warm temperatures. For example, high temperatures shorten times to emergency (Angus et al., 1981), to anthesis (Tompsett, 1976), and the grain filling period (Balasko and Smith, 1971). Several indices have been proposed to quantify the effects of temperature on development rate (Gilmore and Rogers, 1958; Coelho and Dale, 1980).

In EPIC, phenological development of the crop is based on daily heat unit accumulation. It is computed using the equation

$$HU_K = \left(\frac{T_{mx,K} + T_{mn,K}}{2}\right) - T_{b,j} \qquad HU_K > 0 \quad \ldots\ldots\ldots\ldots\ldots\ldots\ldots\ldots\ldots\ldots\ldots\ldots [1]$$

where HU, T_{mx}, and T_{mn} are the values of heat units, maximum temperature and minimum temperature in °C for any day K, and T_b is the crop-specific base temperature in °C (no growth occurs at or below T_b) of crop j. A heat unit index (HUI) ranging from 0 at planting to 1 at physiological maturity is computed as follows.

$$HUI_i = \frac{\left(\sum_{K=1}^{i}\right) HU_K}{PHU_j} \quad \ldots\ldots\ldots\ldots\ldots\ldots [2]$$

where HUI is the heat unit index for day i and PHU is the potential heat units required for maturity of crop j. The value of PHU may be provided by the user or calculated by the model from normal planting and harvest dates. Date of harvest, leaf area growth and senescence, optimum plant nutrient concentrations, and partition of biomass among roots, shoots, and economic yield are affected by HUI.

Potential growth

Interception of solar radiation is estimated with a Beer's law equation (Monsi and Saeki, 1953)

$$PAR_i = 0.5\,(RA)_i\,[1. - \exp(-0.65\,LAI)]_i \quad \ldots\ldots [3]$$

where PAR is intercepted photosynthetic active radiation in $MJ \cdot m^{-2}$, RA is solar radiation in $MJ \cdot m^{-2}$, LAI is the leaf area index, and subscript i is the day of the year. The constant, 0.5, is used to convert solar radiation to photosynthetically-active radiation (Monteith, 1973). Experimental studies indicate that the extinction coefficient varies with foliage characteristics, sun angle, row spacing, row direction, and latitude (Thornley, 1976). The value used in EPIC (0.65) is representative of crops with narrow row spacings (Uchijima et al., 1968). A somewhat smaller value (0.4-0.6) might be appropriate for tropical areas in which average sun angle is higher and for wide row spacings (Begg et al., 1964; Bonhomme et al., 1982; Muchow et al., 1982). Using Monteith's approach (Monteith, 1977), potential increase in biomass for a day can be estimated with the equation

$$\Delta B_{p,i} = 0.001\,(BE)_j (PAR)_i (1 + \Delta HRLT_i)^3 \quad \ldots\ldots [4]$$

where ΔB_p is the daily potential increase in biomass in $t \cdot ha^{-1}$, BE is the crop parameter for converting energy to biomass in $kg \cdot ha \cdot MJ^{-1} \cdot m^2$, HRLT is the daylength in h, and ΔHRLT is the change in daylength in $h \cdot d^{-1}$. The daylength function of equation [4] increases potential growth during the spring and decreases it in the fall. It represents an attempt to mimic the observed, though poorly understood, effects of rate of change of daylength on plant growth (Baker et al., 1980).

Daylength is a function of the time of year and latitude as expressed in the equation

$$HRLT_i = 7.64 \cos^{-1}\left(\frac{-\sin(\frac{2\pi}{360}\,LAT)\,\sin(SD)_i - 0.044}{\cos(\frac{2\pi}{360}\,LAT)\cos(SD)_i}\right) \quad \ldots\ldots [5]$$

where LAT is the latitude of the watershed in degrees and SD, the sun's declination angle, is defined by the equation

$$SD_i = 0.4102 \sin\left(\frac{2\pi}{365}\,(i - 80.25)\right) \quad \ldots\ldots [6]$$

In most crops, leaf area index (LAI) is initially zero or very small. It increases exponentially during early vegetative growth when the rates of leaf primordia development, leaf appearance, and blade expansion are linear functions of heat unit accumulation (Tollenaar et al., 1979; Watts, 1972). In vegetative crops such as sugarcane and some forages, LAI reaches a plateau at which senescence and growth of leaf area approximately equal. In many crops, LAI decreases after the maximum LAI is reached and approaches zero at physiological maturity. In addition, leaf expansion, final LAI, and leaf duration are reduced by stresses (Acevedo et al., 1971; Eik and Hanway, 1965).

LAI is simulated as a function of heat units, crop stress, and crop development stages. From emergence to the start of leaf decline, LAI is estimated with the equations

$$LAI_i = LAI_{i-1} + \Delta LAI \quad \ldots\ldots [7]$$

$$\Delta LAI = (\Delta HUF)(LAI_{mx})\left(1. - \exp(5.(LAI_{i-1} - LAI_{mx}))\right)\sqrt{REG_i} \quad \ldots\ldots [8]$$

where LAI is the leaf area index, HUF is the heat unit factor, and REG is the value of the minimum crop stress factor discussed in more detail below. Subscript mx is the maximum value possible for the crop and Δ is the daily change. The exponential function of equation [8] prevents LAI from exceeding LAI_{mx} when HUF is adjusted for vernalization of certain crops. The heat unit factor is computed using the equation.

$$HUF_i = \frac{HUI_i}{HUI_i + \exp(ah_{j,1} - (ah_{j,2})(HUI_i))} \quad \ldots\ldots [9]$$

Two pairs of values for HUF and HUI are specified as

crop parameters and determine the sigmoid relationship described by equation [9] for crop j. The parameters $ah_{j,1}$ and $ah_{j,2}$ are calculated by simultaneous solution of equation [9] using the two pairs of values for HUF and HUI.

From the start of leaf decline to the end of the growing season, LAI is estimated with the equation

$$LAI_i = LAI_o \left(\frac{1. - HUI_i}{1. - HUI_o} \right)^{ad_j} \quad \ldots\ldots\ldots\ldots [10]$$

where ad is a parameter that governs LAI decline rate for crop j and HUI_o is the value of HUI when LAI starts declining.

Crop height is estimated with the relationship

$$CHT_i = HMX_j \sqrt{HUF_i} \quad \ldots\ldots\ldots\ldots\ldots\ldots [11]$$

where CHT is the crop height in m and HMX is the maximum height for crop j.

The fraction of total biomass partitioned to root system normally decreases from 0.3 to 0.5 in the seedling to 0.05 to 0.20 at maturity (Jones, 1985). The model estimates the fraction of crop growth that is partitioned to the root system to range linearly from 0.4 at emergency to 0.2 at maturity. Thus, the potential daily change in root system weight is computed with the equation

$$\Delta RWT_i = \Delta B_{P,i}(0.4 - 0.2\, HUI_i) \quad \ldots\ldots\ldots\ldots [12]$$

where ΔRWT is the change in root weight in $t \cdot ha^{-1}$ on day i. The distribution of root growth through the root zone is simulated as a function of plant water use in each layer of soil using the equation

$$\Delta RW_{i,\ell} = (\Delta RWT_i) \frac{u_{i,\ell}}{\sum_{\ell=1}^{M} u_{i,\ell}} \quad \ldots\ldots\ldots\ldots [13]$$

where RW is the root weight in soil layer ℓ in $t \cdot ha^{-1}$, M is the total number of soil layers, and u is the daily water use in layer ℓ in mm.

As discussed in the section describing water use, this method of estimating root growth produces realistic exponential decreases in root weight with depth when soil water and other properties do not constrain growth. When a soil layer is dry or root stress factors (strength, aluminum saturation, or aeration) limit root function, both water use and root growth in the layer are reduced.

Rooting depth normally increases rapidly from the seeding depth to a crop-specific maximum. In many crops, the maximum is usually attained well before physiological maturity (Borg and Grimes, 1986). Rooting depth is simulated as a function of heat units and potential root zone depth.

$$RD_i = 2.5(RDMX_j)(HUI_i), \qquad RD_i \leqslant RZ_j \quad \ldots\ldots [14]$$

where RD is the root depth in m, RDMX is the maximum root depth for crop j in ideal soil in m, RZ is the soil profile depth in m, and the constant 2.5 allows root depth to reach its maximum when HUI reaches 0.4.

The economic yield of most grain, pulse, and tuber crops is a reproductive organ. Crops have a variety of mechanisms which insure that their production is neither too great to be supported by the vegetative components nor too small to insure survival of the species. As a result, harvest index (economic yield/above-ground biomass) is often a relatively stable value across a range of environmental conditions. In EPIC, crop yield is estimated using the harvest index concept.

$$YLD_j = (HI_j)(B_{AG}) \quad \ldots\ldots\ldots\ldots\ldots\ldots [15]$$

where YLD is the amount of economic yield that could be removed from the field in $t \cdot ha^{-1}$, HI is the harvest index, and B_{AG} is the above-ground biomass in $t \cdot ha^{-1}$ for crop j. For non-stressed conditions, harvest index increases non-linearly from zero at planting to HI at maturity using the equation

$$HIA_i = HI_j \left(\sum_{K=1}^{i} \Delta HUFH_K \right) \quad \ldots\ldots\ldots\ldots [16]$$

where HIA is the harvest index on day i and HUFH is the heat unit factor that affects harvest index.

The harvest index heat unit factor is computed with the equation

$$HUFH_i = \frac{HUI_i}{HUI_i + \exp(6.50 - 10.0\, HUI_i)} \quad \ldots\ldots\ldots [17]$$

The constants in equation 17 are set to allow $HUFH_i$ to increase from 0.1 at HUI_i=0.5 to 0.92 at HUI_i=0.9. This is consistent with economic yield development of grain crops which produce most economic yield in the second half of the growing season. The effects of stresses on harvest index are discussed in the section on growth constraints.

Water Use

The potential water use, E_p, is estimated as a fraction of the potential evaporation using the leaf-area-index relationship developed by Ritchie (1972).

$$E_{Pi} = E_{oi} \left(\frac{LAI_i}{3} \right), \qquad E_{Pi} \leqslant E_{oi} \quad \ldots\ldots\ldots [18]$$

where E_o is the potential evaporation and LAI is the leaf-area-index on day i.

The potential water use from the soil surface to any root depth is estimated with the function

$$U_{Pi} = \frac{E_{Pi}}{1. - \exp(-\Lambda)} \left(1. - \exp\left(-\Lambda\left(\frac{Z}{RZ}\right)\right) \right) \quad \ldots\ldots [19]$$

where U_p is the total water used in mm to depth Z in m on day i, RZ is the root zone depth in m, and ^ is a water use distribution parameter. The amount used in a particular layer can be calculated by taking the difference between U_{Pi} values at the layer boundaries.

$$u_{P\ell} = \frac{E_{Pi}}{1. - \exp(-\Lambda)} \left(\left(1. - \exp(-\Lambda \left(\frac{Z_\ell}{RZ}\right)) \right) - \left(1. - \exp(-\Lambda \left(\frac{Z_{\ell-1}}{RZ}\right)) \right) \right) \quad \ldots\ldots\ldots\ldots [20]$$

where $u_{p\ell}$ is the potential water use from layer ℓ in mm. Equation 20 represents a soil that provides poor conditions for root development when Λ is set a high value like 10. The high Λ value gives high water use near the surface and very low use in the lower half of the root zone. Since there is no provision for water deficiency compensation in any layer, considerable water stress may result using equation [20]. To overcome this problem, equation [20] was modified to allow plants to compensate for water deficiency in a layer by using more water from other layers. Total compensation can be accomplished by taking the difference between U_{Pi} at the bottom of a layer and the sum of water use above a layer.

$$u_{P\ell} = \frac{E_{Pi}}{1. - \exp(-\Lambda)} \left(1. - \exp(-\Lambda \left(\frac{Z_\ell}{RZ}\right)) \right) - \sum_{K=1}^{\ell-1} u_K \quad \ldots\ldots\ldots\ldots\ldots\ldots\ldots\ldots [21]$$

where u_K is the actual water use in mm for all layers above layer ℓ. Thus, any deficit can be overcome if a layer is encountered that has adequate water storage. Neither equation [20] (no compensation) nor equation [21] (total compensation) is satisfactory to simulate a wide range of soil conditions. A combination of the two equations, however, provides a very general water use function.

$$u_{P\ell} = \frac{E_{Pi}}{1. - \exp(\Lambda)} \left(1. - \exp(-\Lambda \left(\frac{Z_\ell}{RZ}\right)) - (1. - UC) \left(1. - \exp(-\Lambda \left(\frac{Z_{\ell-1}}{RZ}\right)) \right) \right) - UC \sum_{K=1}^{\ell-1} u_K \quad \ldots\ldots\ldots\ldots\ldots\ldots\ldots\ldots [22]$$

where UC ranges (0.0 to 1.0) and is the water deficit compensation factor. In soils with a good rooting environment, UC=1. gives total compensation. The other extreme, poor conditions, allow no compensation (UC=0.). The procedure for estimating UC is described in the Growth Constraints section.

The potential water use in each layer (neglecting the effects of root constraints) calculated with equation [22] is reduced when the soil water storage is less than 25% of plant-available soil water (Jones and Kiniry, 1986) using the equation.

$$u_\ell = u_{P\ell} \exp \left(5. \left(\frac{4.(SW_{\ell i} - WP_\ell)}{(FC_\ell - WP_\ell)} - 1. \right) \right), \quad SW_{\ell i} < \frac{FC_\ell - WP_\ell}{4.} + WP_\ell \quad \ldots\ldots\ldots\ldots [23]$$

$$u_\ell = u_{P\ell}, \quad SW_\ell \geqslant \frac{FC_\ell - WP_\ell}{4.} + WP_\ell \quad \ldots\ldots [24]$$

where SW is the soil water content in layer ℓ on day i in mm and FC and WP are the soil water contents at field capacity and wilting point for layer ℓ.

Nutrient uptake

Nitrogen

Crop use of N is estimated using a supply and demand approach. The daily crop N demand is the difference between the crop N content and the ideal N content for day i. The demand is estimated with the equation

$$UND_i = (c_{NB})_i (B)_i - \sum_{K=1}^{i=1} UN_K \quad \ldots\ldots\ldots\ldots [25]$$

where UND is the N demand of the crop in $kg \cdot ha^{-1}$, UN is the actual N uptake in $kg \cdot ha^{-1}$, c_{NB} is the optimal N concentration of the crop in $kg \cdot t^{-1}$, and B is the accumulated biomass in $t \cdot ha^{-1}$ for day i. The optimal crop N concentration declines with increasing growth stage (Jones, 1983a) and is computed as a function of growth stage using the equation

$$c_{NBi} = bn_1 + bn_2 \exp(-bn_3 \, HUI_i) \quad \ldots\ldots\ldots\ldots [26]$$

where HUI (heat unit index) is the fraction of the growing season and bn_1, bn_2, and bn_3 are parameters calculated from crop-specific concentrations of N in the plant at the seedling stage, halfway through the season, and at maturity.

Mineral nutrients move to plant roots primarily by mass flow and diffusion. Mass flow is the movement of nutrients to roots in the soil water absorbed and transpired by the plant. Mass flow rarely provides exactly the amount of nutrient absorbed by the plant; therefore, the concentration of nutrient near the root may increase or decrease in response to the balance between mass flow and absorption (Barber, 1984). Diffusion causes the nutrient concentration gradient between the root to the bulk soil to decrease, and when soil solution concentrations are low it can provide a significant fraction of N absorbed by the plant. Barber (1984) suggests that mass flow normally accounts for about 80% of the N uptake of corn roots, and a combination of mass flow and diffusion can reduce soil NO_3—N to very low levels.

In EPIC, mass flow of NO_3—N to the roots is used to distribute potential N uptake among soil layers

$$UN_{\ell,i} = u_{\ell,i} \left(\frac{WNO3_\ell}{SW_\ell} \right)_i \quad \ldots\ldots\ldots\ldots\ldots\ldots [27]$$

where UN is the amount of N supplied by the soil in $kg \cdot ha^{-1}$, WNO3 is the amount of NO_3—N in $kg \cdot ha^{-1}$, SW is the soil water content in mm, u is water use in mm, and subscript ℓ refers to the soil layers. The total N available for uptake by mass flow is estimated by summing mass flow of all layers.

$$UNS_i = \sum_{K=1}^{M} UN_{\ell,i} \quad \ldots\ldots\ldots\ldots\ldots\ldots [28]$$

Since mass flow rarely provides the exact amount of N required by the crop, UN values obtained from equation [27] are adjusted.

$$UNa_{\ell,i} = UN_{\ell,i} \left(\frac{UND_i}{UNS_i}\right), \qquad UNa_{\ell,i} \leqslant WNO3_{\ell,i} \quad [29]$$

where UNa is the adjusted N supply in $kg \cdot hg^{-1}$ for layer ℓ. Equation 29 assures that actual N uptake cannot exceed the plant demand when mass flow exceeds demand. It also provides for increased N supply from the layer (by diffusion) when mass flow does not meet crop demand but NO_3—N is available in the soil.

Nitrogen Fixation: Daily N fixation is estimated as a fraction of daily plant N demand by legumes.

$$WFX_i = FXR_i \cdot UND_i, \qquad WFX \leqslant 6.0 \quad [30]$$

where WFX is the amount of N fixation in $kg \cdot ha^{-1}$ and FXR is the fraction of uptake for day i. The fraction, FXR, is estimated as a function of soil NO_3 and water content and plant growth stage.

$$FXR = \min (1.0, FXW, FXN) \cdot FXG \quad [31]$$

where FXG is the growth stage factor, FXW is the soil water content factor, and FXN is the soil NO_3 content factor. The growth stage factor inhibits N fixation in young plants prior to development of functional nodules and in old plants with senescent nodules (Patterson and LaRue, 1983).

$$FXG_i = 0.0, \qquad HUI_i \leqslant 0.15, \ HUI \geqslant 0.75 \quad [32]$$

$$FXG_i = 6.67\ HUI_i - 1.0, \qquad 0.15 < HUI_i \leqslant 0.3 \quad [33]$$

$$FXG_i = 1.0, \qquad 0.3 < HUI_i \leqslant 0.55 \quad [34]$$

$$FXG_i = 3.75 - 5.0\ HUI_i, \qquad 0.55 < HUI_i < 0.75 \quad [35]$$

where HUI is the heat unit index for day i. The soil water content factor reduces N fixation when the water content at the top 0.3 m is less than 85% of field capacity (Albrecht et al., 1984; Bouniols et al., 1985) using the equation

$$FXW_i = \frac{SW3_i - WP3}{0.85\ (FC3 - WP3)},$$

$$SW3 < 0.85\ (FC3 - WP3) + WP3 \quad [36]$$

where SW3, WP3, and FC3 are the water contents in the top 0.3 m of soil on day i, at wilting point, and at field capacity.

The amount of NO_3 in the root zone can affect N fixation (Harper, 1976; Bouniols et al., 1985) determines the soil NO_3 factor, FXN.

$$FXN = 0., \qquad WNO3 > 300.\ kg \cdot ha^{-1} \cdot m^{-1} \quad [37]$$

$$FXN = 1.5 - 0.005 \left(\frac{WNO3}{RD}\right), \qquad 100. < WNO3 \leqslant 300. \quad [38]$$

$$FXN = 1.0, \qquad WNO3 \leqslant 100.\ kg \cdot ha^{-1} \cdot m^{-1} \quad [39]$$

Where WNO3 is the weight of NO_3—N in the root zone in $kg \cdot ha^{-1}$ and RD is the root depth in m. This approach reduces N fixation when the NO_3—N content of the root zone is greater than 100 $kg \cdot ha^{-1}$ and prohibits N fixation at N contents greater than 300 $kg \cdot ha^{-1}$.

Phosphorus

Crop use of P is estimated with the supply and demand approach described in the N model. The daily plant demand is computed with equation [25] written in the form

$$UPD_i = (c_{PB})_i (B)_i - \sum_{K=1}^{i-\ell} UP_K \quad [40]$$

where UPD is the P demand for the plant in $kg \cdot ha^{-1}$, UP is the actual P uptake in $kg \cdot ha^{-1}$, and c_{PB} is the optimal P concentration for the plant. As in the case of N, the optimal plant P concentration is computed with equation [26] in written in the form

$$c_{PBi} = bp_1 + bp_2 \exp(-bp_3\ HUI_i) \quad [41]$$

where bp_1, bp_2, and bp_3 are parameters calculated from crop-specific optimum P concentrations at the seedling stage, halfway through the season and at maturity. Soil supply of P is estimated using the equation

$$UPS_i = 1.5\ UPD_i \sum_{\ell=1}^{M} (LF_u)_\ell \left(\frac{RW_\ell}{RWT_i}\right) \quad [42]$$

where UPS is the amount of P supplied by the soil in $kg \cdot ha^{-1}$, LF_u is the labile P factor for uptake, RW is the root weight in layer ℓ in $kg \cdot ha^{-1}$, and RWT is the total root weight on day i in $kg \cdot ha^{-1}$. The constant 1.5 allows 2/3 of the roots to meet the P demand of the plant if labile P is not limiting. This approach is consistent with studies suggesting that roots of P-deficient plants (or plants whose root systems have been pruned) can absorb P faster than the roots of normal plants (Andrews and Newman, 1970; DeJager, 1979; Jungk and Barber, 1974).

The labile P factor for uptake ranges from 0.1 to 1.0 according to the equation

$$LF_{u\ell} = 0.1 + \frac{0.9\ c_{LP\ell}}{c_{LP\ell} + 117. \exp(-0.283\ c_{LP\ell})} \quad [43]$$

where c_{LP} is the labile P concentration in soil layer ℓ in $g \cdot t^{-1}$. Equation 43 allows optimum uptake rates when c_{LP} is above 20 $g \cdot t^{-1}$. This is consistent with critical labile P concentrations for a range of crops and soils (Sharpley et al., 1989). Sharpley et al. (1984, 1985) described methods of estimating c_{LP} from soil test P and other soil characteristics.

Growth Constraints

Potential crop growth and yield are usually not achieved because of constraints imposed by the plant environment. The model estimates stresses caused by water, nutrients, temperature, aeration, and radiation. These stresses range from 0.0 to 1.0 and affect plants in several ways. In EPIC, the stresses are considered in estimating constraints on biomass accumulation, root growth, and yield. The biomass constraint is the minimum of the water, nutrient, temperature, and aeration stresses. The root growth constraint is the minimum of soil strength, temperature, and aluminum toxicity. Though topsoil aluminum toxicity can have a direct effect on shoot growth, EPIC simulates only its indirect effects through its inhibition of root growth and water use. A description of the stress factors involved in determining each constraint follows.

Biomass

The potential biomass predicted with equation [4] is adjusted daily if any of the five plant stress factors is less than 1.0 using the equation

$$\Delta B = (\Delta B_p)\,(REG) \quad \ldots\ldots\ldots\ldots\ldots\ldots [44]$$

where REG is the crop growth regulating factor (the minimum stress factor).

Water Stress: The water stress factor is computed by considering supply and demand in the equation

$$WS_i = \frac{\sum_{\ell=1}^{M} u_{i,\ell}}{E_{Pi}} \quad \ldots\ldots\ldots\ldots\ldots\ldots [45]$$

where WS is the water stress factor, u is the water use in layer ℓ, and E_p is the potential plant water use on day i. This is consistent with the concept that drought stress limits biomass production in proportion to transpiration reduction (Hanks, 1983).

Temperature Stress: The plant temperature stress is estimated with the equation

$$TS_i = \sin\left(\frac{\pi}{2}\left(\frac{T_{gi} - T_{bj}}{T_{oj} - T_{bj}}\right)\right), \quad 0 \leqslant TS_i \leqslant 1 \quad \ldots\ldots [46]$$

where TS is the plant temperature stress factor T_g is the average daily soil surface temperature in °C, T_b is the base temperature for crop j, and T_o is the optimal temperature for crop j. Equation [46] produces symmetrical plant growth stress about the optimal temperature and it is driven by average daily soil surface temperature. This approach allows growth of small plants to respond realistically to low soil surface temperatures found in temperate regions in the spring. The presence of soil residues can retard simulated soil warming and reduce crop growth. As the crop canopy develops, it shades the soil surface, and simulated average soil surface temperature approaches average air temperature. A more detailed description of the soil temperature model is given in Williams et al. (1984).

Nutrient Stress: The N and P stress factors are based on the ratio of simulated plant N and P contents to the optimal values. The stress factors vary non-linearly from 1.0 at optimal N and P contents to 0. when N or P is half the optimal level (Jones, 1983a). In the case of N, the scaling equation is

$$SN_{S,i} = 2\left(1 - \frac{\sum_{K=1}^{i} UN_K}{(c_{NB})_i (B)_i}\right) \quad \ldots\ldots\ldots\ldots [47]$$

where SN_S is a scaling factor for the N stress factor, c_{NB} is the optimal N concentration of the crop on day i, B is the accumulated biomass in kg·ha^{-1}, and UN is the crop N uptake on day K in kg·ha^{-1}. The N stress factor is computed with the equation

$$SN_i = 1 - \frac{SN_{S,i}}{SN_{S,i} + \exp(3.39 - 10.93\, SN_{S,i})} \quad \ldots\ldots [48]$$

where SN is the N stress factor for day i. The P stress factor is computed with equations [47] and [48] written in P terms.

Aeration Stress: When soil water content approaches saturation, plants may suffer from aeration stress. The water content of the top 1 m of soil is considered in estimating the degree of stress.

$$SAT = \frac{SWI}{POI} - CAF_j \quad \ldots\ldots\ldots\ldots\ldots\ldots [49]$$

$$AS_i = 1. - \frac{SAT}{SAT + \exp(-1.291 - 56.1\, SAT)}, \quad SAT > 0.0$$

$$\ldots\ldots\ldots\ldots\ldots\ldots\ldots\ldots [50]$$

where SAT is the saturation factor, SW1 is the water content of the top 1 m of soil in mm, PO1 is the porosity of the top 1 m of soil in mm, CAF is the critical aeration factor for crop j ($\approx$0.85 for many crops), and AS is the aeration stress factor. This approach allows the model to restrict crop growth both when water tables are high (but a layer of aerated soil occurs near the surface) and when slow internal drainage causes poor aeration near the soil surface. Several studies suggest that when water-filled pore space (WFP) exceeds 60% (Linn and Doran, 1984; Grable and Seimer, 1968; Trouse, 1964), root growth is inhibited by poor aeration. EPIC produces similar results when CAF=0.85, WFP exceeds 60% in the surface 0.5 m, and the soil is saturated from 0.5 to 1.0 m. Growth of flood-tolerant crops like rice can be simulated by setting CAF=1.0.

Finally, the value of REG is determined as the minimum of WS, TS, SN, SP, and AS.

Root Growth

As described in equation [13], root growth is proportional to water use. Water use from a soil layer is estimated as a function of soil depth, water content, and a compensation factor using equation [22] and [23]. Soil strength, temperature, and aluminum toxicity stress factors are calculated from soil properties. The minimum of these three stresses, the root growth stress

factor, constains root growth by governing the water use compensation factor.

Cold soil temperature may limit root growth, especially when subsoil layers warm slowly in the spring (Taylor, 1983). Temperature stress for each soil layer is computed by substituting soil temperature at the center of the layer for soil surface temperature in equation [46].

Numerous studies have shown that root growth is affected by soil strength. Three important strength determinants are bulk density, texture, and water content (Eavis, 1972; Monteith and Banath, 1965; Taylor et al., 1966). All three of these variables are considered in estimating the EPIC soil strength stress factor using the following equation.

$$SS_{\ell} = 0.1 + \frac{0.9\ BD_{\ell}}{BD_{\ell} + \exp(bt_1 + bt_2(BD_{\ell}))} \quad \ldots\ldots [51]$$

where SS is the soil strength factor in layer ℓ, BD is the soil bulk density adjusted for water content in $t \cdot m^{-3}$, and bt_1 and bt_2 are parameters dependent upon soil texture. The values of bt_1 and bt_2 are obtained from a simultaneous solution of equation [51] by substituting boundary conditions for stress. The lower boundary where essentially no stress occurs is given by the equation (Jones, 1983b)

$$BDL = 1.15 + 0.00445\ SAN \quad \ldots\ldots [52]$$

where BDL is the bulk density near the lower boundary (SS=1.) for a particular percent sand, SAN. The upper boundary is given by equation (Jones, 1983b)

$$BDU = 1.5 + 0.05\ SAN \quad \ldots\ldots [53]$$

where BDU is the bulk density near the upper boundary (SS≈0.2) for a particular percent sand, SAN. The equations for estimating bt_1 and bt_2 are

$$bt_2 = \frac{\ln(0.112\ BDL) - \ln(8.\ BDU)}{BDL - BDU} \quad \ldots\ldots [54]$$

$$bt_1 = \ln(0.0112\ BDL) - (bt_2)(BDL) \quad \ldots\ldots [55]$$

Equations [54] and [55] assure that equation [51] gives SS values of 1.0 and 0.2 for BD equal BDL and BDU (Jones, 1983b).

The water-content adjusted bulk density used in equation [51] is estimated with Grossman's equation (Grossman et al., 1985)

$$BD_{\ell,i} = BD3 + (BDD - BD3)\left(\frac{FC_{\ell} - SW_{\ell,i}}{FC_{\ell} - WP_{\ell}(4.083 - 3.33\ BDD^{1/3})}\right) \quad \ldots\ldots [56]$$

where BD is the water content adjusted bulk density on day i, BD3 is the bulk density at 33 kPa water content, BDD is the oven dry bulk density, FC is the field capacity, WP is the wilting point, and SW is the soil water content for layer ℓ on day i.

Aluminum (Al) toxicity can limit root growth in some acid soil layers, and Al saturation is a widely used index of its effects (Abruna et al., 1982; Brenes and Pearson, 1973; Pavan et al., 1982). Because crops and cultivars differ in their sensitivities to Al toxicity (Foy et al., 1972, 1974; Mugwira et al., 1980), EPIC considers both the Al toxicity of the soil and crop sensitivity to it. Root growth stress caused by aluminum toxicity is estimated with the equation

$$ATS_{\ell} = \frac{1}{100 - ALO_j}, \qquad ALS_{\ell} > ALO_j \quad \ldots\ldots [57]$$

$$ATS_{\ell} = 1.0, \qquad ALS_{\ell} \leqslant ALO_j \quad \ldots\ldots [58]$$

where ATS is the aluminum toxicity root growth stress factor for soil layer ℓ, ALS is the aluminum saturation in %, and ALO is the maximum ALS value crop j can tolerate without stress in %. Crop specific values of ALO are determined from the equation

$$ALO_j = 10 + 20(ALT_j - 1) \quad \ldots\ldots [59]$$

where ALT_j is the aluminum tolerance index number for crop j. Values of ALT range from 1 to 5 (1 is sensitive; 5 is tolerant) for various crops. Finally, the root growth stress factor, RGF, is the minimum of SS, ATS, and TS.

Water use

Plant water use is governed by the root growth stress factor using the water deficit compensation factor of equation [22]. Recall that the water deficit compensation factor, UC, allows total compensation if the value is 1.0 and no compensation at 0.0. The value of UC for any layer is estimated as the product of the root growth stress factors for the layer and all layers above.

$$UC_{\ell} = \sum_{K=1}^{\ell} RGF_K \quad \ldots\ldots [60]$$

Thus, a low RGF_K greatly reduces water compensation for layer K and all layers below K. The final estimates of water use for each layer are obtained by multiplying the equations [23] and [24] u_{ℓ} values by RGF.

$$u^*_{\ell} = (u_{\ell})(RGF)_{\ell} \quad \ldots\ldots [61]$$

Crop Yield

Crop yield may be reduced through reductions in harvest index caused by water stress. Most grain crops are particularly sensitive to water stress from shortly before until shortly after anthesis, when major yield components are determined (Doorenbos and Kassman, 1979). Optimum conditions for growth may reduce harvest index slightly if dry matter accumulation is large and economic yield is limited by sink size. The harvest index is affected by water stress using the equation

$$HIA_i = HIA_{i-1} - HI_j\left(1 - \frac{1}{1 + (WSYF_j)(FHU_i)(0.9 - WS_i)}\right) \quad \ldots\ldots [62]$$

where HI_j is the normal harvest index for crop j, HIA is the adjusted harvest index, $WSYF_j$ is a crop parameter expressing the sensitivity of harvest index to drought for crop j, FHU is a function of crop growth stage, and WS is the water stress factor for day i. Notice that harvest index may increase slightly on days with WS values greater than 0.9. The crop stage factor, FHU, is estimated with the equation

$$FHU_i = \sin\left(\frac{\pi}{2}\left(\frac{HUI_i - 0.3}{0.3}\right)\right), \quad 0.3 \leqslant HUI_i \leqslant 0.9 \quad [63]$$

when

$FHU_i = 0., \; HUI_i < 0.3$

or

$HUI_i > 0.9$

Thus, water stress only affects harvest index between 0.3 and 0.9 of maturity with the greatest effect occurring at 0.6.

Winter Dormancy

The daylength growth constraint is used to simulate a winter dormant period for fall planted crops. These constraints are only imposed for areas that have less than 12 months growing season. A 12-month growing season for warm-season crops is defined in the model as one that has no months with mean minimum temperature less than 5°C. If there is a dormant winter period, it is defined as the time when daylength is within 1 h of the location's minimum daylength.

If a crop experiences a winter dormant period, the heat unit summation (equation [2]) is set to zero. This provides for rapid new growth when temperatures increase in the spring. During the dormant period, the plants are not allowed to grow. The standing live biomass is actually decreased during this period due to frost and short daylength. The daylength reduction factor is estimated with the equation

$$FHR_i = 0.35\left(1.0 - \frac{HRLT_i}{HRLT_{mn} + 1.}\right) \quad [64]$$

where FHR is the daylength reduction factor, HRLTi is the daylength on day i, and HRLTmn is the minimum daylength for the location. The frost reduction factor is estimated with the equation

$$FRST_i = \frac{-T_{mn,i}}{-T_{mn,i} - \exp(af_{j,1} + af_{j,2} \cdot T_{mn,i})},$$

$$T_{mn,j} < 1. \; °C \quad [65]$$

where $FRST_i$ is the frost damage factor, T_{mn} is the minimum temperature on day i in °C, and $af_{j,1}$ and $af_{j,2}$ are parameters expressing the crop's frost sensitivity. The reduction in standing live biomass is estimated with the equation

$$\Delta B_{AG,i} = 0.5 \cdot B_{AG,i}(1.0 - HUI_i) \cdot \max(FHR_i, FRST_i) \quad [66]$$

where Δ_{BAG} is the reduction in above ground in $t \cdot ha^{-1}$ on day i, HUI is the heat unit index, and B_{AG} is the above ground biomass in $t \cdot ha^{-1}$ on day i. Note that frost damage is greater when plants are small (HUI≈0)and approaches zero near maturity.

MODEL TESTING

The model was tested with data from several locations with considerable variation in soil and weather

TABLE 1. Data For Rice, Sunflower, Barley and Soybean Used for Yield Demonstration of the EPIC Model

Crop	Location	Years	Researchers
Corn	Yuma, AZ	1974	Stewart et al. (1977)
	Davis, CA	1974-1975	Stewart et al. (1977)
	Fort Collins, CO	1974-1975	Stewart et al. (1977)
	Logan, UT	1974-1975	Stewart et al. (1977)
	Mandan, ND	1968-1970	Alessi and Power (1977)
	Florence, SC	1980-1982	Karlen and Camp (unpubl.)
	Temple, TX	1979	Pietsch and Gerik (1980)
	Bushland, TX	1975-1977	Musick and Dusek (1980)
	Story, Ringgold, and Monona, IA	1960-1970	Laflen (unpubl.)
Wheat	Phoenix, AZ	1977-1978	Dusek (unpubl.)
	Garden City, KS	1980-1981	Wagger (1983)
	Hutchinson, KS	1979-1980	Wagger (1983)
	Manhattan, KS	1981	Wagger and Kissel (unpubl.)
	Pendleton, OR	1980-1981	Klepper et al. (1983)
	Bushland, TX	1977	Musick and Dusek (unpubl.)
	Temple, TX	1977	Monk, Arkin, Maas, and Ritchie (unpubl.)
	Lind, WA	1976	Johnson (1978)
	Pullman, WA	1972	Thill (1976)
Rice	Far East, Southeast Asia, Southern Asia, South America	1983-1984	Oldeman et al., (1986)
Sunflowers, Barley, Soybeans	Toulouse, France	1983-1986	INRA, Toulouse, France (unpubl.)
Soybeans	Ringgold, IA	1963-1969	Laflen (unpubl.)

characteristics (Table 1). The tests involved were: (1) the response of corn (*Zea mays* L.) grain yield to soil depth for three locations; (2) measured and simulated grain yields for six crop species in a wide range of environments; (3) the ability of the model to simulate corn yield response to irrigation for four arid locations in the U.S.; and (4) the ability of the model to simulate N-response for six corn planting dates in Hawaii.

Materials and Methods

General

EPIC requires a number of crop-specific inputs. Once these input paramaters were set for a crop species, they were not adjusted for individual data sets or locations. however, potential heat units from planting to maturity may vary at different locations for the same crop.

In all but two cases, the water balance was simulated using the Penman method (Penman, 1956) of estimating potential evaporation. In testing the rice (*Oryza sativa* L.) yields and in testing the N-response of corn in Hawaii, lack of wind data necessitated use of the Priestley-Taylor equation (Priestley and Taylor, 1972; Ritchie, 1972).

Simulating Corn Grain Yield Response to Decreased Soil Depth

The purpose of this test was to demonstrate EPIC's ability to simulate the effect of soil depth on corn yield. Three locations with a range in annual rainfall were chosen for the test (Columbia, MO — 970 mm; Temple, TX — 860 mm; and Bushland, TX — 460 mm). The same silt loam soil was used at all three locations. Soil characteristics were assumed uniform throughout the 940 mm soil profile depth (bulk density=1.4 $t \cdot m^{-3}$, wilting point=0.16 $m \cdot m^{-1}$, field capacity=0.315 $m \cdot m^{-1}$, sand=20%, silt=70%, and pH=7.0). For each location, grain yield was predicted for 13 consecutive years of generated weather. The first three years were used to remove the effect of initial estimates of soil water and NO_3. Thus, only results from the last 10 years were used in the analysis. Three simulations were performed using the same weather and the same soil, except 7, 14, or 22 cm of soil was removed from the bottom of the 94 cm soil profile. Removal was from the bottom of the profile to standardize the top layers across depth treatments. The surface layer was 15 cm in all cases. Each soil profile was given a runoff curve number appropriate for its total depth.

Simulating Grain Yield of Six Crop Species

Several statistics were used to evaluate the model's effectiveness in estimating yields for six crops at various locations. First the means and standard deviations of the measured and simulated yields were compared. Close agreement in mean and standard deviation indicates similarity in yield probability distributions. Yield probability distributions are useful in decision making. For each crop, a paired comparison t-test was used to determine if the difference between measured and predicted values was significantly different from zero (SAS, 1982).

Model performance was evaluated further by regressing simulated on measured yields. The first aspect of this approach was to check for a significant relationship between simulated and measured yields. This consisted of testing whether the slope of the regression line was significantly different from zero. If it was not, the model failed to show superiority over simply using the mean measured yield for prediction.

If the regression line had a significant positive slope, it was compared with the ideal line through the origin with a slope of 1.0. The simulations were checked for bias by constructing a confidence band for the regression line and checking to see if the ideal line was outside this band.

Finally, the r^2 provided a final means of describing how well the simulated and measured yields agreed.

Simulating Corn Grain Yield Response to Irrigation

These simulations were designed to test the model's ability to simulate yield under various soil moisture conditions. The data came from a four-location, two-year study with a wide range of irrigation levels and measured yields (Stewart et al., 1977). The high evaporative demand at these sites was desirable for testing the water balance. Simulated yields were graphically compared to measured yields.

N-Response of Corn in Hawaii

The ability of EPIC to simulate N-response for corn grain yields was tested for four planting dates at one location and one planting at each of two others, all in Hawaii. The soil at all locations was Hydric Dystrandept. For each planting, there were six nitrogen treatments ranging from zero to a maximum of between 185 and 225 kg/ha. Based on description of the data (Singh, 1985), the initial organic N in the soil was between 0 and 30 tons/ha throughout the profile. Within this range, initial organic N values were adjusted to give reasonable simulation of humus mineralization. Close agreement between measured and simulated yields for the 0 applied N treatment indicates proper humus mineralization simulation. The simulated yields for all the treatments were then graphically compared to the measured yields.

TABLE 2. Pertinent Crop Parameters Used in the EPIC Runs

Parameter	Crop					
	Corn	Wheat	Rice	Sunflower	Soybeans	Barley
BE	40.0	35.0	20.0	60.0	25.0	25.0
HI	0.50	0.42	0.50	0.25	0.31	0.42
T_o	25.0	15.0	24.0	25.0	25.0	15.0
T_b	8.0	0.0	8.0	6.0	10.0	0.0
LAI_{mx}	5.0	8.0	6.5	5.0	9.0	7.0
HUI_o	0.80	0.80	0.78	0.55	0.60	0.75
ah_1	15.05	15.01	20.01	15.01	15.01	15.01
ah_2	50.95	50.95	70.95	50.95	50.95	50.95
af_1	5.01	5.01	1.50	5.15	5.01	5.01
af_2	15.05	15.10	2.95	15.95	15.05	15.10
ad_j	1.00	1.00	0.50	1.00	1.00	1.00
ALT	3.0	2.0	3.0	3.0	3.0	1.0
CAF	0.85	0.85	1.0	0.85	0.85	0.85
HMX	2.5	1.2	0.8	2.5	1.5	1.2
RDMX	2.0	2.0	0.9	2.0	2.0	2.0
WSYF	0.050	0.010	0.010	0.010	0.010	0.010
bn_1	0.044	0.060	0.05	0.05	0.0524	0.06
bn_2	0.0164	0.0231	0.0200	0.0230	0.0320	0.0231
bn_3	0.0128	0.0134	0.0100	0.0146	0.0286	0.0130
bp_1	0.0062	0.0084	0.0060	0.0063	0.0074	0.0084
bp_2	0.0023	0.0032	0.0030	0.0029	0.0037	0.0032
bp_3	0.0018	0.0019	0.0018	0.0023	0.0035	0.0019

TABLE 3. Values for PHU for Various Locations and Years Unless Otherwise Noted, the Values were Input

Crop	Location	PHU
Corn	Florence, SC	2000
	Bushland, TX	2000
	Columbia, MO	1820
	Mandan, ND	1020*
	Bloomington, IL	1970*
	Logan, UT	1625
	Davis, CA	1760
	Fort Collins, CO	1205
	Yuma, AZ	2835*
	Manona, IA	1730-1830*
	Story, IA	1670-1830*
	Ringgold, IA	1850-2000*
Wheat	Pullman, WA	1790-2690*
	Pendleton, OR	1710-1962*
	Garden City, KS	1614-1835*
	Hutchinson, KS	1463*
	Manhattan, KS	1942*
	Bushland, TX	1650-1965*
	Temple, TX	1502*
	Phoenix, AZ	1485-2346*
Rice	Cuttack, India	2100
	Coimbatore, India	2100
	Kapurthala, India	2100
	Nanjing, China	2100
	Muara, Indonesia	2100
	Parwanipur, Nepal	2100
	Sakha, Egypt	2100
	Suweon, South Korea	2100
	Milyang, South Korea	2100
	Ahero, Kenya	1600
	Palmira, Columbia	1600
	Pintung, China	1600
	Sanpatong, Thailand	1600
	Los Banos, Philippines	1600
	Masapang, Philippines	1600
Sunflower	France	1442-1849*
Soybeans	France	1123-1282*
	Ringgold, IA	1576*
Barley	France	1524-2000*

Results

General

As discussed above, a number of input values were required to describe each crop (Tables 2 and 3). Definitions of parameters are given in Appendix A. Only the potential heat units (PHU) from planting to maturity varied among cultivars within a species. Thus, while the number of these inputs was great, only one was adjusted for the proper cultivar for a location.

Most PHU values for corn were input, but some were calculated by the model using average temperatures between planting and harvest (Table 3). In the latter case, harvesting was assumed to occur at maturity. The PHU for corn ranged from 1020 C for Mandan, ND, to 2835 C for Yuma, AZ. The PHU for wheat (*Triticum aestivum* L.) was calculated in all cases and ranged from 1463 to 2690 C.

Wetland rice, partially because of its unusual soil environment, was often the divergent species for a parameter. Noteworthy cases were for the two points on the leaf area development curve, ah_1 and ah_2; the second point was the frost damage curve, af_2; the critical aeration factor, CAF; and maximum rooting depth, RDMX (Appendix A).

Rice was also unusual in that all the values for PHU were input. A preliminary test of the data indicated that the values for PHU from planting to reported dates of maturity fell into two divergent groups. The means for the two groups were approximately 2100 C and 1600 C. Thus, these values were used for the simulations. It was interesting to note that with only two exceptions, all the locations in the 2100 C PHU group were at latitudes greater than 20°. Those in the 1600 C PHU group, with one exception, were at latitudes less than 20°. The variety of IR36 is sensitive to photoperiod, with a 7.5 d delay in flower per hour increase in photoperiod above 14 hours (Vergara and Chang, 1985). Thus, photoperiod probably was at least partially responsible for the differences in development rate at the different latitudes.

Values for PHU of sunflower (*Helianthus annus* L.), soybeans (*Glycine max* (L.) Merr.), and barley (*Hordeum vulgare* L.) were calculated based on the reported harvest dates. These values can be used for further applications of EPIC when the harvest date is not reported.

Simulating Corn Grain Yield Response to Decreased Soil Depth

The response of yield to reduced soil depth was dependent on amount of rainfall (Fig. 1). Mean simulated yields tended to decline as the soil profile was reduced at Columbia and Temple, but such a tendency was not evident at Bushland. Thus, the soil water holding capacity of the profile was a limitation only at the first two locations. Even a profile of 72 cm was deep enough to accommodate the limited water at Bushland.

Perhaps the most noteworthy aspect of this analysis was the magnitude of the variability associated with each mean yield as evidenced by the large LSD values. At all three locations, yields were not significantly different among soil depths. Previously, the effect of weather on grain yield reduced yield prediction accuracy using a productivity index (Kiniry et al., 1983). Thus, a process-oriented, weather-dependent model appears to be a more feasible means for quantifying yield response to erosion.

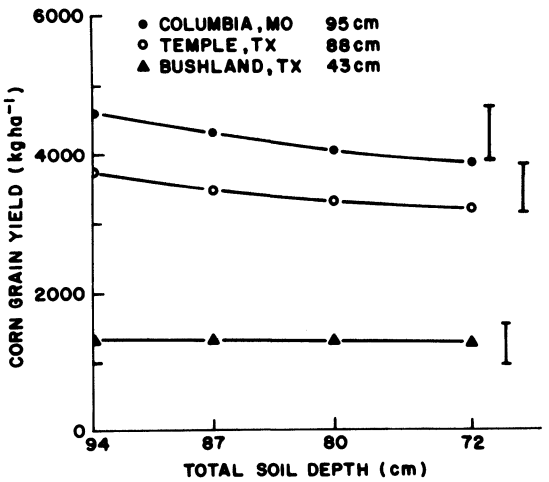

Fig. 1—Simulated response of corn yield to reduced soil depth for three locations.

TABLE 4. Mean and Standard Deviation of Measured and Simulated Yield for the Six Crop Species

Crop	N	Yield				t-values for differences in means†
		Measured		Simulated		
		$\bar{x}$	SD	$\bar{x}$	SD	
		(tons/ha)				
Corn	118	6.5	3.1	6.3	3.1	-1.0
Wheat	20	3.8	2.1	3.7	1.8	-0.5
Rice	33	5.6	1.7	5.3	1.3	-1.1
Sunflower	27	2.9	0.9	2.7	0.9	-1.4
Barley	19	3.5	1.2	3.3	0.7	-0.8
Soybeans	10	2.1	0.4	2.2	0.3	0.7

†None were significant at the 95% confidence level.

Simulating Grain Yield of Six Crop Species

EPIC's mean simulated yields were always within 7% of the mean measured yields (Table 4). With the exception of the soybean simulations, mean simulated yield of each crop was greater than the mean measured value. The wheat crop had the smallest percent difference between mean simulated and measured yields, while sunflower had the greatest. None of the crops had a significant difference between measured and simulated mean yields.

The SDs of the simulated yields were similar to the SDs of the measured, but the percent differences between simulated and measured SDs were greater (up to 34% for barley) in general than for the means. Two exceptions to this were corn and sunflower, with 0 and 4% differences in SD, respectively.

EPIC simulated corn yields reasonably in the high, intermediate, and low yielding conditions (Fig. 2). The slope of the regression line was less than 1.0. Measured yields ranged from zero in some dryland studies in the southwestern U.S. to almost 14 t·ha^{-1} at two irrigated sites. The slope was significantly different from zero at the 95% confidence level. The value of r^2 was high (0.65) and the fitted line was close to the 1:1 line. The 1:1 line fell well within the 95% confidence band for the regression line.

Results with wheat were similar to those with corn. There was a wide range of measured yields, with some less than 1 t·ha^{-1} and one of 9 t·ha^{-1}. Again, there was a significant relationship between measured and predicted yield. The value of r^2 was 0.80 and the fitted line fell within the 95% confidence band for the regression line. Measured wheat yields in both the high and low yielding environments were simulated reasonably well. However, similar to corn the slope of the regression line was less than 1.0. This indicated that the model was not as responsive to the environment as it should have been.

Data for rice (*Oryza sativa* (L.)) was a subset from a multilocation wetland study done by IRRI (Oldeman et al., 1986). These data were collected at locations in the Philippines, Asia, Africa, and South America. Testing was done using 33 of the original 63 data sets. Those not included had unusual problems with pests or disease, unusual management practices, or some other anomaly. Only data for the standard variety IR36 were included. However, two values for PHU were used as discussed above. As in the previous two comparisons, there was a significant relationship between measured and simulated yields. The value of r^2 was not as high, 0.41, but the 1:1 line was within the 95% confidence band except in the extreme upper range of the data. The simulated yields tended to be less than the measured yields in the higher yielding environments. However, EPIC simulated the second highest measured yield nearly exactly. Again, the low value for the slope of the regression line, 0.48, implied that the model was not as responsive to the environment as it should have been.

Simulated yields of sunflower were also significantly related to the measured yields. The r^2, 0.42, was similar to the value for rice. The regression line was close to the 1:1 line and within the 95% confidence band throughout the range of the data. Simulated yields were similar to measured yields at both the lowest and the highest values.

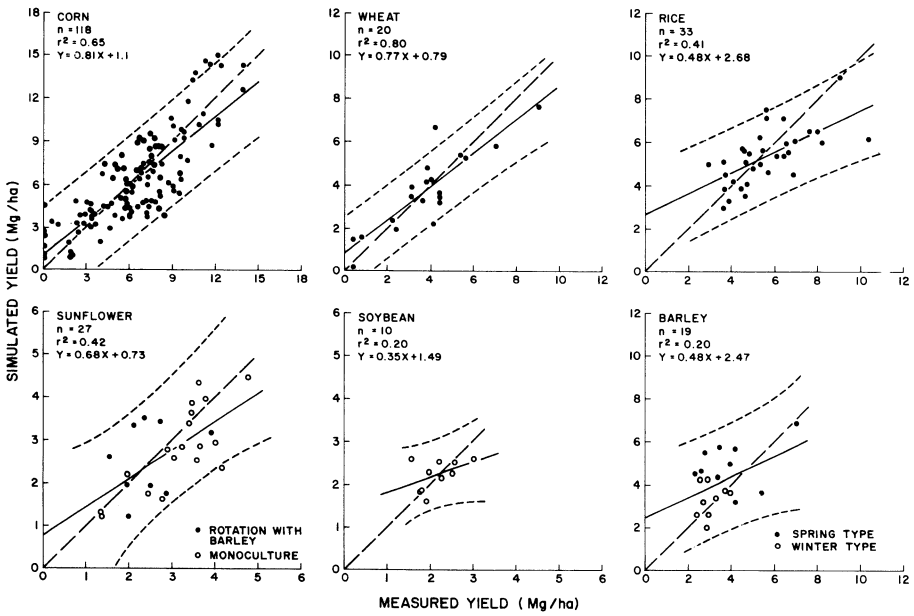

Fig. 2—Simulated and measured yield of six crop species.

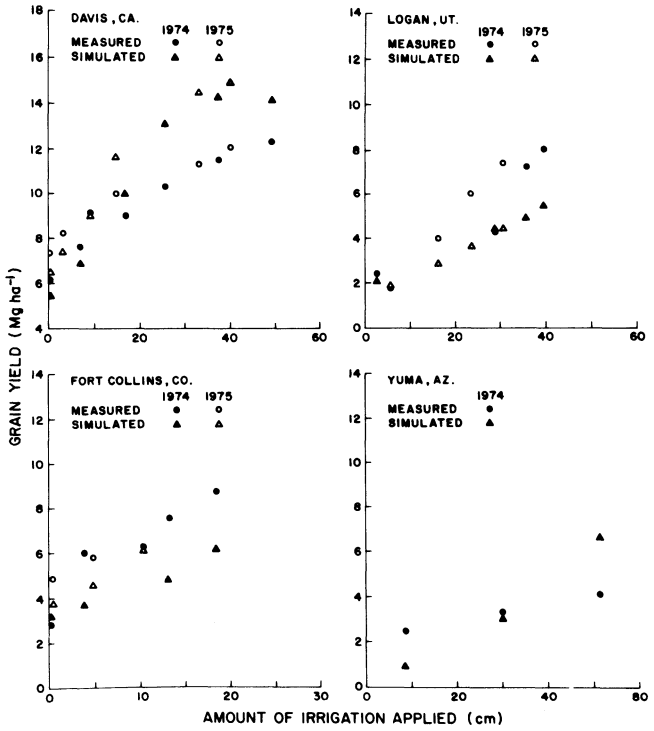

Fig. 3—Simulated response of corn yield to irrigation for four locations.

The small range of measured yields of soybeans and barley restricted the amount of variability the model could account for and thus restricted the r^2. Soybean yields ranged from 1.5 to 3.0 t·hd^{-1}, and barley yields ranged from 2.4 to 4.2 t·ha^{-1}, excluding the two highest yielding data sets. Slopes for the simulated:measured regression line were not significantly different from zero for either crop. The values for r^2 were low 0.20 — for both cases. However, there was no obvious bias in simulated yields and the 1:1 line fell within the confidence band for both crops. EPIC, therefore, failed to account for the variability in yield of these two crops but gave a reasonable average yield.

Simulating Corn Grain Yield Response to Irrigation

Simulated corn yield response to irrigation was similar to measured response from Davis, CA (Fig. 3). At the lowest values, the model tended to slightly underpredict grain yield. In contrast the high yielding treatments were slightly overpredicted. However, in general, EPIC simulated the effects of water stress on grain yield at this location reasonably well.

Simulations of corn yield at Logan, UT were close to measured yields in the lowest irrigation treatments. Similar to the results at Davis, the model showed a yield response throughout the range of irrigation levels. However, the simulated yields were less than the measured values in the high yielding treatments.

Simulations of corn yield at Fort Collins, CO, were closer to measured values in 1975 than in 1974. In all but the lowest yielding treatment in 1974, measured yield was considerably greater than simulated. It appeared that the simulated evaporative demand was too great or the input soil water holding capacity was too low in 1974.

Finally, EPIC overestimated yield response to irrigation in Yuma, AZ, in 1974. Measured yields were increased only 1.6 t·ha^{-1} while the model simulated a 5.6 t·ha^{-1} increase. However both simulated and measured yields showed some yield response throughout the range of irrigation treatments.

N-Response of Corn in Hawaii

Generally, simulated yields were similar to measured throughout the range of N application (Fig. 4). In addition, for up to about 100 kg/ha applied-N, both simulated and measured yields increased with increased applied N. However, the model usually failed to adequately simulate the plateau in response at the upper range of applied N values.

The measured yield showed a plateau in the response above approximately 110 to 130 kg·ha^{-1} applied-N in

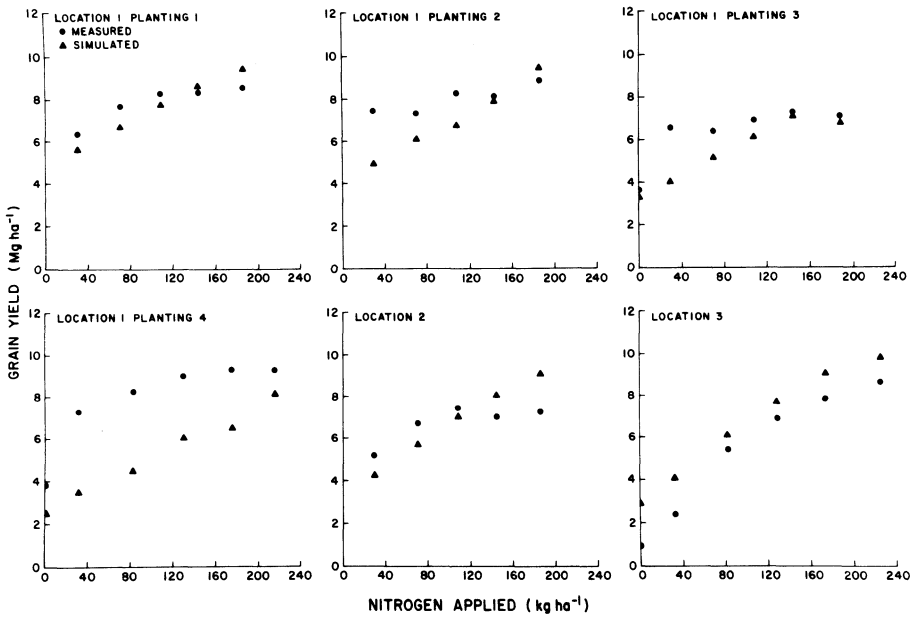

Fig. 4—Simulated response of corn yield to applied-nitrogen for six plantings in Hawaii.

planting 1, 2, and 4 of location 1 and at location 2. However, in all these cases, the simulated yield continued to increase up to the maximum amount of applied-N. Thus, the model overestimated the impact of applied-N on yield above about 120 $kgN \cdot ha^{-1}$ application.

Two cases where the measured and simulated yield responded similarly at the high N application rates were location 1, planting 3 and location 3. In the first situation, measured and simulated yields increased with an increase in applied N up to 135 $kg \cdot ha^{-1}$ N, with a slight decrease at the greatest amount of applied-N. Likewise for location 3, both measured and simulated showed very similar increases in yield for each additional increment of applied-N, throughout the range of treatments.

SUMMARY AND CONCLUSIONS

The EPIC plant growth model was developed to estimate soil productivity as affected by erosion throughout the U.S. Since soil productivity is expressed in terms of crop yield, the model must be capable of simulating crop yields realistically for soils with a wide range of erosion damage. Also, simulations of many crops are required because of the wide variety grown in the U.S.

To meet the requirements, a general crop model that is sensitive to the plant environment (climate, nutrient supply, and soil characteristics) was developed. The EPIC crop parameter table presently contains parameters for about 25 crops. Parameters for other crops may be obtained from experts or from the literature.

The plant growth model has been tested throughout the U.S. and in several foreign countries. The simulation of crop yield by EPIC predicted the response of long-term yield to various management strategies. Mean simulated yields for crops and the associated standard deviations were remarkably close to values for measured yields. None of the simulated means were significantly different from the measured means at the 95% confidence level. Likewise, there was a significant ($\alpha = 0.05$) relationship between measured and simulated yields for all crops except soybeans and barley.

EPIC also accurately simulated corn yield response to irrigation; thus, it could be used for irrigation scheduling. However, the regression lines of predicted yield as a function of measured yield for the various crops consistently had slopes less than 1.0. This indicated that the model was not as responsive to the environment as it should have been. These errors could be especially important when making real-time irrigation or fertilizer application decisions. Similar results at Bushland, TX (Steiner et al., 1987) indicated that EPIC is best suited for making long-term management decisions.

References

1. Abruna, F., J. Rodriquez and S. Silva. 1982. Crop response to soil acidity factors in Ultisols and Oxisols in Puerto Rico. VI. Grain sorghum. *J. Agric. Univ. of Puerto Rico* 61:28-38.

2. Acevedo, E., T.C. Hsiao and D.W. Henderson. 1971. Immediate and subsequent growth responses of maize leaves to changes in water status. *Plant Physiol.* 48:631-636.

3. Albrecht, S.L., J.M. Bennett and K.J. Boote. 1984. Relationship of nitrogenase activity to plant water stress in field-grown soybeans. *Field Crops Res.* 8:61-71.

4. Alessi, J. and J.F. Power. 1975. Effects of plant population, row spacing and relative maturity on dryland corn in the northern plains. I. Corn forage and grain yield. *Agron. J.* 66:316-319.

5. Andrews, R.E. and E.I. Newman. 1970. Root density and competition for nutrients. *Oecol. Plant.* 5:319-334.

6. Angus, J.F. 1981. Phasic development in field crops. I. Thermal response in the seedling phase. *Field Crops Res.* 3:365-378.

7. Baker, C.K., J.N. Gallagher and J.L. Monteith. 1980. Daylength change and leaf appearance in winter wheat. *Plant, Cell and Environ.* 3:285-287.

8. Balsko, J.A. and D. Smith. 1971. Influence of temperature and nitrogen fertilization on the growth and composition of switchgrass (*Panicum virgatum* L.) and timothy (*Phleum pratense* L.) at anthesis. *Agron. J.* 63:853-857.

9. Barber, S.A. 1984. *Soil nutrient bioavailability.* New York: John Wiley & Sons, Inc.

10. Begg, J.E. 1964. Diurnal energy and water exchanges in bulrush millet in an area of high solar radiation. *Agric. Meteorol.* 1:294-312.

11. Bonhomme, R., F. Ruget, M. Derieux and P. Vincourt. 1982. Relations entre production de matiere seche aerienne et energie interceptee chez differents genotypes de mais. *C.R. Acad. Sci. Paris* 294:393-398.

12. Borg, H. and D.W. Grimes. 1986. Depth development of roots with time: An empirical description. *Transactions of the ASAE* 29(1):194-197.

13. Bouniois, A. et al., 1985. Influence des conditions d'alimentation hydrique ou (et) azotee a differents stades du developpement sur la production de grains et la nutrition azotee du soja. *Eurosoya* 3:55-61.

14. Brenes, E. and R.W. Pearson. 1973. Root responses of three Gramineae species to soil acidity in an Oxisol and an Ultisol. *Soil Sci.* 116:295-302.

15. Coelho, D.T. and R.F. Dale. 1980. An energy-crop growth variable and temperature function for predicting corn growth and development: Planting to silking. *Agron. J.* 72:503-510.

16. DeJager, A. 1979. Localized stimulation of root growth and phosphate uptake in *Zea mays* L. resulting from restricted phosphate supply. pp. 391-403. *In* J.L. Harley and R. Scott Russell, eds. *The Soil-Root Interface.* New York: Academic Press.

17. Doorenbos, J. and A.H. Kassam. 1979. *Yield response to water.* Irrigation and Drainage Paper 33. Food and Agric. Org. of the United Nations, Rome.

18. Eavis, B.W. 1972. Soil physical conditions affecting seedling root growth. I. Mechanical impedance, aeration, and moisture availability as influenced by bulk density and moisture levels in a sandy loam soil. *Plant Soil* 36:613-622.

19. Eik, K. and J.J. Hanway. 1965. Some factors affecting development and longevity of leaves of corn. *Agron. J.* 57:7-12.

20. Foy, C.D., A.L. Fleming and G.C. Gerloff. 1972. Differential aluminum, tolerance in two snapbean varieties. *Agron. J.* 64:815-818.

21. Foy, C.D. et al., 1974. Aluminum tolerance of wheat cultivars related to region of origin. *Agron. J.* 66:751-758.

22. Gilmore, E.C. and J.S. Rogers. 1958. Heat units as a method of measuring maturity in corn. *Agron. J.* 50:611-615.

23. Grable, A.R. and E.G. Seimer. 1968. Effects of bulk density, aggregate size and soil water suction on oxygen diffusion, redox potential and elongation of corn roots. *Soil Sci. Soc. Amer. Proc.* 32:180-186.

24. Grossman, R.B., W.D. Nettleton and B.R. Brasher. 1985. Application of pedology to plant response prediction for tropical vertisols. In *Proc. Fifth Int. Soil Classification Workshop,* Sudan, November 2-11, 1982.

25. Hanks, R.J. 1983. Yield and water-use relationships: An overview. pp. 393-411. In H.M. Taylor, W.R. Jordan and T.R. Sinclair, eds. *Limitations to Efficient Water use in Crop Production.* Amer. Soc. Agron., Crop Sci. Soc. Amer., Soil Sci. Soc. Amer., Madison, WI.

26. Harper, J. E. 1976. Contribution of dinitrogen and soil or fertilizer nitrogen to soybean (*Glycine max* L. Merr.) production. p. 101-107. In L. D. Hill, ed. *World soybean research conference.* Danville, ILL: The Interstate Printers and Publishers, Inc.

27. Johnson, R.C. 1978. Apparent photosynthesis and evapotranspiration of winter wheat in a field environment. M.S. thesis, Washington State Univ., Pullman.

28. Jones, C.A. 1983a. A survey of the variability in tissue nitrogen and phosphorus concentrations in maize and grain sorghum. *Field Crops Res.* 6:133-147.

29. Jones, C.A. 1983b. Effect of soil texture on critical bulk densities for root growth. *Soil Sci. Soc. Amer. J.* 47:1208-1211.

30. Jones, C.A. 1985. *C-4 grasses and cereals.* New York: John Wiley & Sons, Inc.

31. Jones, C.A. and J.R. Kiniry, eds. 1986. *CERES-Maize.* College Station: Texas A&M Univ. Press.

32. Jones, C.A., A. N. Sharpley and J. R. Williams 1984a. A simplified soil and plant phosphorus model: I. Documentation. *Soil Sci. Soc. Amer. J.* 48:800-805.

33. Jones, C.A., A.N. Sharpley and J.R. Williams. 1984b. A simplified soil and plant phosphorus model: III. Testing. *Soil Sci. Soc. Amer. J.* 48:800-805.

34. Jungk. A. and S.A. Barber. 1974. Phosphate uptake of corn roots as related to the proportion of the roots exposed to phosphate. *Agron. J.* 66:554-557.

35. Kiniry, L.N., C.L. Scrivner and M.E. Keener. 1983. *A soil productivity index based upon predicted water depletion and root growth.* Univ. Missouri Agric. Exp. Sta. Res. Bull. 1051, 26p.

36. Klepper, B., T.W. Tucker and B.D. Dunbar. 1983. A numerical index to assess early inflorescence development in wheat. *Crop Sci.* 23:206-208.

37. Linn, D.M. and J.W. Doran. 1984. Effect of water-filled pore space on carbon dioxide and nitrous oxide production in tilled and nontilled soils. *Soil Sci. Soc. Amer. J.* 48:1267-1272.

38. Monsi, M. and T. Saeki. 1953. Uber den Lichfaktor in den Pflanzengesellschaften und sein Bedeutung fur die Stoffproduktion. *Japan J. Bot.* 14:22-52.

39. Monteith, J.L. 1973. *Principles of Environmental Physics.* London: Edward Arnold.

40. Monteith, J.L. 1977. Climate and the efficiency of crop production in Britain. *Phil. Trans. Res. Soc. London B.* 281:277-329.

41. Monteith, N.H. and C.L. Banath. 1965. The effect of soil strength on sugarcane growth. *Trop. Agric.* 42:293-296.

42. Muchow, R.C. et al., 1982. Growth and productivity of irrigated *Sorghum bicolor (*L. Moench) in Northern Australia. I. Plant density and arrangement effects of light interception and distribution, and grain yield, in the hybrid Texas 610SR in low and medium latitudes. *Aust. J. Agric. Res.* 33:773-784.

43. Mugwira, L.M., S.J. Patel and A.L. Fleming. 1980. Aluminum effects on growth and Al, Ca, Mg, K, and P levels in triticale, wheat, and rye. *Plant Soil* 57:467-470.

44. Musick, J.T. and D.A. Dusek. 1980. Irrigated corn yield response to water. *Transactions of the ASAE* 23(1):92-98, 103.

45. Oldeman, L.R., D.V. Seshu and F.B. Cady. 1986. *Response of rice to weather variables.* Intl. Rice Res. Inst. Report. Manila, Philippines.

46. Patterson, T.G. and T.A. LaRue. 1983. Nitrogen fixation by soybeans: Cultivar and seasonal effects of comparison of estimates. *Crop Sci.* 23:488-492.

47. Pavan, M.A., F.T. Bingham and P.F. Pratt. 1982. Toxicity of aluminum to coffee in Ultisols and Oxisols amended with $CaCO_3$, $MgCO_3$, and $CaSO_4 \cdot 2H_2O$. *Soil Sci. Soc. Amer. J.* 46:1201-1207.

48. Penman, H.L. 1956. Evaporation: An introductory survey. *Neth. J. Agric. Sci.* 4:9-29.

49. Pietsch, D. and T.J. Gerik. 1980. *Corn hybrid performance.* Texas Agric. Exp. Sta. Bull. PR3724, 13p.

50. Priestley, C.H.B. and R.J. Taylor. 1972. On the assessment of surface heat flux and evaporation using large-scale parameters. *Mon. Weather Rev.* 100:81-92.

51. Ritchie, J.T. 1972. A model for predicting evaporation from a row crop with incomplete cover. *Water Resources Res.* 8:1205-1213.

52. SAS Institute. 1982. *SAS User's Guide: Statistics.* SAS Inst., Cary, NC, 584.

53. Sharpley, A.N. et al., 1984. A simplified soil and plant phosphorus model: II. Prediction of labile, organic, and sorbed phosphorus. *Soil Sci. Soc. Amer. J.* 48:800-805.

54. Sharpley, A.N. et al., 1985. A detailed phosphorus characterization of seventy-eight soils. ARS-31. 32 p.

55. Sharpley, A.N., C.A. Jones and J.R. Williams. 1989. The nutrient submodel of EPIC. In A.N. Sharpley and J.R. Williams, eds. *The Erosion-Productivity Impact Calculator (EPIC).* (in press). Model Documentation.

56. Singh, U. 1985. A crop growth model for predicting corn performance in the tropics. Ph.D. diss., Univ. Hawaii.

57. Steiner, J.L., J.R. Williams and O.R. Jones. 1987. Evaluation of the EPIC simulation model using a dryland wheat-sorghum-fallow crop rotation. *Agron. J.* 79:732-738.

58. Stewart, J.I. et al., 1977. *Optimizing crop production through control of water and salinity levels in the soil.* Utah Water Res. Lab. PRWG 151-1. 191 p.

59. Taylor, H.M. 1983. A program to increase plant available water through rooting modification. pp. 463-472. In *Root Ecology and Its Practical Application.* Int. Symp., Gumpenstein. September 27-29, 1982. Budndesanstalt fur alpenlandische Landwirtschalf, A-8952 Irding.

60. Taylor, H.M., G.M. Robertson and J.J. Parker, Jr. 1966. Soil strength — Root penetration relations for medium to coarse-textured soil materials. *Soil Sci.* 102:18-22.

61. Thill, D.C. 1976. Physiological and environmental effects on yield potential in early- and late-planted winter wheat. M.S. thesis, Washington State Univ., Pullman.

62. Tollenaar, M., T.B. Daynard and R.B. Hunter. 1979. Effect of temperature on rate of leaf appearance and flowering date of maize. *Crop Sci.* 19:363-366.

63. Thornley, J. H. M. 1976. *Mathematical models in plant physiology.* London: Academic Press.

64. Tompsett, P.B. 1976. Factors affecting the flowering of *Andropogon gayanus* Kunth. Responses to photoperiod, temperature, and growth regulators. *Ann. Bot.* 40:695-705.

65. Trouse, A.C., Jr. 1964. Effects of compression of some subtropical soils on the soil properties and upon root development. Ph.D. dis., Univ. Hawaii, Honolulu.

66. Vergara, B.S. and T.T. Chang. 1985. *The flowering response of the rice plant to photoperiod.* Intl. Rice Res. Inst., Manila. 61 p.

67. Wagger, M.G. 1983. Nitrogen cycling in the plant-soil system. Ph.D. thesis, Kansas State Univ., Manhattan.

68. Watts, W.R. 1972. Leaf extension in *Zea mays*. II. Leaf extension in response to independent variation of the temperature of the apical meristem, of the air around the leaves, and of the rootzone. *J. Exp. Bot.* 23:713-721.

69. Williams, J.R., C.A. Jones and P.T. Dyke. 1984. A modeling approach to determining the relationship between erosion and soil productivity. *Transactions of the ASAE* 27(1)1:129-144.

APPENDIX A

Notation

Λ	plant water use rate-soil depth parameter
af_1,af_2	crop parameters for frost sensitivity
ah_1,ah_2	crop parameters that determine the shape of the leaf-area-index development curve
ad	crop parameter that governs leaf area index decline rate
ALO	maximum ALS value a crop can tolerate without stress (%)
ALS	aluminum saturation of the soil(%)
ALT	aluminum tolerance index number
AS	aeration root growth stress factor (0-1)
ATS	aluminum toxicity root growth stress factor (0-1)
bn_1,bn_2,bn_3	crop parameters for plant N concentration equation
bp_1,bp_2,bp_3	crop parameters for plant P concentration equation
bt_1,bt_2	soil strength parameters related to soil texture
B	accumulated plant biomass (above ground and roots) ($t \cdot ha^{-1}$)
B_{AG}	above ground biomass of growth crop ($t \cdot ha^{-1}$)
B_P	potential crop biomass ($kg \cdot ha^{-1}$)
BD	soil bulk density ($t \cdot m^{-3}$)
BDD	oven dry soil bulk density ($t \cdot m^{-3}$)
BD3	33 kPa water content bulk density ($t \cdot m^{-3}$)
BDL	bulk density near lower boundary of stress (causes no root growth stress) ($t \cdot m^{-3}$)
BDU	bulk density near upper stress boundary (root growth stress ≈ 0.2 ($t \cdot m^{-3}$)
BE	crop parameter — converts energy to biomass ($kg \cdot ha \cdot MJ^{-1} \cdot m^{-2}$)
c_{LP}	labile P concentration in the soil ($g \cdot t^{-1}$)
c_{NB}	optimal N concentration for a plant ($g \cdot g^{-1}$)
c_{PB}	optimal P concentration for a plant ($g \cdot g^{-1}$)
CAF	critical aeration factor for a crop
CHT	crop height (m)
CLA	clay content of the soil (%)
E_o	potential evaporation ($mm \cdot d^{-1}$)
E_P	potential plant evaporation rate ($mm \cdot d^{-1}$)
FC_1	field capacity (33 kPa for many soils) water content of soil layer 1 (mm)
FHU	crop stage (heat unit) factor governing water stress-harvest index

FHR	winter dormancy day length factor for reducing standing live biomass (0-1)
FRST	frost damage factor (0-1)
HI	potential harvest index — ratio of crop yield to above ground biomass
HIA	actual harvest index for a crop
HMX	maximum crop height (m)
HRLT	daylength (h)
HU	daily heat units — average daily temperature minus base temperature of crop (°C)
HUF	heat unit factor for driving leaf-area-index development (0-1)
HUFH	heat unit factor for estimating harvest index development (0-1)
HUI	heat unit index — ratio of accumulated to potential heat units (0-1)
HUI_o	heat unit index value when leaf area index starts declining
LAI	leaf area index — area of plant leaves relative to the soil surface
LAI_{mx}	maximum LAI potential for a crop
LAI_o	leaf area index value at start of decline
LAT	latitude of watershed (degrees)
LF_u	labile P factor for crop uptake (0-1)
PAR	photosynthetically active radiation ($MJ \cdot m^{-2}$)
PHU	potential heat units for a crop (°C)
RA	solar radiation (ly)
RAF	solar radiation factor affecting harvest index
RD	root depth (m)
RDMX	maximum root depth for a crop (m)
REG	crop growth constraint (minimum stress factor — water, nutrients, aeration, temperature)
RGF	root growth constraint (minimum stress factor — soil strength, temperature, aluminum toxicity)
RW_1	root weight in soil layer 1 ($t \cdot ha^{-1}$)
RWT	total root weight ($t \cdot ha^{-1}$)
RZ	root zone depth (m)
SAN	sand content of a soil layer (%)
SAT	saturation index for top 1 m of soil
SD	sun's declination angle (radians)
SN	N stress factor for crop growth (0-1)
SN_S	N stress scaling factor
SS	soil strength root growth stress factor (0-1)
SW_1	soil water content in layer 1 (mm)
t	time (h)
T	temperature (°C)
T_b	base temperature for a crop (plants start growing) (°C)
T_g	soil surface temperature (°C)
T_{mn}	daily minimum air temperature (°C)
T_{mx}	daily maximum air temperature (°C)
T_o	optimal temperature for a crop (°C)
TH	temperature stress factor affecting harvest index (0-1)
TS	temperature stress factor for crop growth (0-1)
u_1	plant water use rate in soil layer 1 ($mm \cdot d^{-1}$)
u_{p1}	potential plant water use rate in soil layer ($mm \cdot d^{-1}$)
UN_1	N supply rate in layer 1 ($kg \cdot ha^{-1} \cdot d^{-1}$)
U_P	daily potential plant water use from the root zone (mm)
UC	soil water deficit compensation factor (0-1)
UN	N uptake rate of plant ($kg \cdot ha^{-1} \cdot d^{-1}$)
UND	plant N demand rate ($kg \cdot ha^{-1} \cdot d^{-1}$)
UNS	N supply rate of soil ($kg \cdot ha^{-1} \cdot d^{-1}$)
UP	P uptake rate of plant ($kg \cdot ha^{-1} \cdot d^{-1}$)
UPD	plant demand rate ($kg \cdot ha^{-1} \cdot d^{-1}$)
UPS	P supply rate of soil ($kg \cdot ha^{-1} \cdot d^{-1}$)
WNO_3	weight of NO_3 in a soil layer ($kg \cdot ha^{-1}$)
WP_1	soil water content of layer 1 at wilting point (mm)
WS	water stress factor for crop growth (0-1)
WSYF	water stress factor for adjusting harvest index
YLD	crop yield ($t \cdot ha^{-1}$)
Z	soil depth from the surface (m)